Title
THE CRACK-TIP DISPLACEMENT CONCEPT APPLIED TO COMPOSITES

Author
Gerberich, W.W.

Publication Date
1968-12-01

UCRL-18660
cy. 2

THE CRACK-TIP DISPLACEMENT CONCEPT APPLIED TO COMPOSITES

William W. Gerberich

December 1968

LAWRENCE RADIATION LABORATORY
UNIVERSITY of CALIFORNIA BERKELEY

UCRL-18660
cy. 2

DISCLAIMER

Submitted to the Journal
of Materials Science

UCRL-18660
Preprint

UNIVERSITY OF CALIFORNIA
Lawrence Radiation Laboratory
Berkeley, California
AEC Contract No. W-7405-eng-48

THE CRACK-TIP DISPLACEMENT CONCEPT APPLIED TO COMPOSITES

W. W. Gerberich

December 1968

THE CRACK-TIP DISPLACEMENT CONCEPT APPLIED TO COMPOSITES

William W. Gerberich

Inorganic Materials Research Division, Lawrence Radiation Laboratory, Department of Materials Science and Engineering, College of Engineering, University of California, Berkeley, California

ABSTRACT

An investigation of ductile fiber fracture in a unidirectional composite indicates that a critical crack-tip displacement or fracture strain concept may be utilized to predict fracture. Crack-propagation tests in an aluminum alloy reinforced with stainless-steel wires were evaluated for 0.05, 0.10 and 0.20 volume fraction composites. Measurement of the average stress intensity factor occurring during fiber breakage was accomplished with the aid of a stress-wave detection system. This allowed the discontinuous crack steps associated with fiber breakage to be monitored and thus allowed a particular load for a particular fiber break to be established. The fracture strain associated with fiber breakage was established metallographically from measurements of the necked-down region at the fractured ends of the fibers. For all volume fractions, the average calculated fracture strain was 1.07 as compared to the average measured value of 0.93.

THE CRACK-TIP DISPLACEMENT CONCEPT APPLIED TO COMPOSITES

William W. Gerberich

Inorganic Materials Research Division, Lawrence Radiation Laboratory, Department of Materials Science and Engineering, College of Engineering, University of California, Berkeley, California

1. INTRODUCTION

Many continuum approaches to fracture have been developed in the last twenty years including stress concentration, stress intensity and strain energy release rate (modified Griffith) concepts. However, there has been limited use of these in the understanding of how to make materials more resistant to fracture. For this reason, one of the most exciting developments is that of the crack-tip displacement concept since it presents the possibility of relating the structural unit involved in fracture to some microstructural characteristic.

For example, Cottrell[1] and Tetelman and McEvily[2] have proposed a critical crack-tip displacement concept in terms of a micro-tensile sample fracturing at the crack tip. The length of the sample is limited by the root radius of the crack and the width is limited by those microstructural factors which limit ductility. Taking the fracture strain to be exceeded over the dimensions of the micro-tensile sample, one can easily visualize a brittle second phase rod fracturing ahead of the main crack. This has actually been observed in a two-phase macrocomposite of brittle tungsten wires in a 2% Be-Cu matrix.[3] Alternatively, a ductile rod at the crack tip could be visualized to neck down considerably before fracture. Indeed, in a current study[4] on a composite with a ductile, strong stainless steel wire in an age-hardened aluminum matrix, the 0.0091 inch (0.23 mm) diameter wires failed in a cup-cone fashion as a micro-tensile sample. Since the reduction of area of the wires was sufficiently large to allow estimates of the fracture ductility, it seemed that this could provide a reasonable check of the crack-tip displacement concept.

The criterion as put forth by Cottrell and Tetelman is

$$2v_c^* = 2\rho\epsilon^* \tag{1}$$

where $2v_c^*$ is the critical crack-tip displacement, ρ is the crack-tip radius and ϵ^* is the fracture strain of the micro-tensile sample. Those parameters which affect v_c also affect ρ. Therefore, it is difficult to check this concept in terms of Eq. (1).

Another way of utilizing the concept, although in a slightly modified vein, is to assume that the fracture strain is exceeded over some critical distance, ℓ^*, in front of the crack. This criterion may actually be derived without the use of the crack-tip displacement concept. First, consider that at large stress intensities there is plastic flow through the thickness of a thin plate and so plane stress conditions prevail. McClintock[5] has described the strain distribution in front of a crack undergoing longitudinal shear. Gerberich[6] has demonstrated that the tensile analogy is a reasonable approximation to the experimentally determined strain distributions about a crack under tensile stresses. The strain distribution is given by

$$\epsilon_1 = \frac{\sigma_{ys}}{E} \frac{R_p}{\ell} \tag{2}$$

where ϵ_1 is the maximum principal strain, σ_{ys} is the yield strength, E is the modulus of elasticity, R_p is the plastic zone diameter and ℓ is the distance in front of the crack tip. McClintock[7] has suggested that the distance from the crack to the elastic-plastic boundary be given in terms of the stress intensity factor, K, by

$$R_p = \frac{K^2}{\pi\sigma_{ys}^2} \tag{3}$$

If one assumes that fracture may occur over a distance ℓ^* where the maximum principal strain is greater than or equal to the fracture ductility, ϵ^*, then a combination of Eqs. (2) and (3) leads to

$$\epsilon^* = \frac{K^2}{\pi\sigma_{ys}E\ell^*} \tag{4}$$

The same equation may be achieved considering the crack-tip displacement. Wells[8] has shown the relationship between ℓ^*, ϵ^* and the crack-tip displacement to be

$$\ell^* = \frac{2v_c}{\pi\epsilon^*} \tag{5}$$

Hahn and Rosenfield[9] have expressed the crack-tip displacement in terms of the stress intensity factor by

$$2v_c = \frac{K^2}{\sigma_{ys}E} \tag{6}$$

Combining equations (5) and (6) leads to

$$\ell^* = \frac{K^2}{\pi\sigma_{ys}E\epsilon^*} \tag{7}$$

which is identical to Eq. (4). Thus, with the point of view taken herein, the critical strain and critical displacement criterions are interchangeable. It is now useful to consider how this concept might apply to the observations made on an aluminum-steel composite.

2. RESULTS AND DISCUSSION

Unidirectional composites were purchased commerically[†] in the form of 0.1 inch (2.54mm) thick plate with volume fractions of 0.05, 0.10, 0.20 and 0.40. The composites consisted of 450,000 psi (315 kg/mm^2) stainless steel wire in a 68,000 psi (47.5 kg/mm^2) aluminum alloy matrix having the following compositions:

(wt.%)	C	Mo	Ni	Cr	Mn	Si	Fe	Cu	Zn	Mg
N355 stainless steel wire (0.009 in. diam.)	0.13	2.85	4.5	15.5	0.75	0.35	bal.			
2024 T-4 Aluminum				0.1	0.6	0.5	0.5	4.4	0.25	1.5

Micrographs of three different volume fractions are shown in Fig. 1. Uniaxial tensile evaluations parallel to the reinforcement provided the relationship between strength and volume fraction shown in Fig. 2. Since the matrix work-hardened considerably prior to fracture, the theoretical curve using the ultimate strength of the matrix fit the data best in Fig. 2.

Single-edge notch specimens were utilized to study a crack growing across the wires. A crack-line loaded sample was chosen since this provides about a 10:1 mechanical advantage with respect to failing the specimen in uniaxial tension. For this reason, there is no danger of failing the specimen at the loading pin holes. The specimen configuration, which was essentially 2.0 inches (51 mm) wide by 3.0 inches

---

[†]Harvey Aluminum, Torrance, California

(76 mm) high, is indicated in Fig. 3. Knowing the load (P) the specimen thickness (B) width (W) and crack length (a), the stress intensity can be determined from

$$K = \frac{P}{BW^{1/2}} f\left(\frac{a}{w}\right) \tag{8}$$

where f(a/w) as given in Fig. 3 is taken from the numerical solution of Srawley and Gross.[10] The height of the specimen was not always the same due to material availability, but W/Hp did stay within the limits indicated in Fig. 3.

Specimens were pulled at a crosshead speed of 0.1cm/min. and load-time recordings were made to maximum load, at which point specimens were unloaded for metallographic examination. Examples of fractures are shown for three different volume fractions in Fig. 4. It was observed that the crack would progress in the matrix; a wire would fracture; the matrix would crack again and then another wire would fracture. Thus, it was assumed that as the crack arrived at the matrix wire interface, the fracture of the wire necessitated the fracture strain to be exceeded over the entire wire diameter. As the wires necked considerably before the fracture, the average neck diameter was taken as the value of ℓ^* over which the fracture strain had to be exceeded. This is depicted in Fig. 5. The value of ℓ^* was measured from the photomicrographs. Also determined was the stress intensity value at which wire fracture occurred. This was accomplished with the assistance of a stress-wave technique[11] to detect crack growth. Every time a wire fractured, an elastic wave with a well-defined amplitude was emitted and recorded. The set-up for accomplishing this is schematically shown in Fig. 6. Essentially, the voltage signal from the accelerometer is amplified by the charge amplifier, filtered to cut out extraneous mechanical noises, further amplified to drive a damped galvanometer with high frequency response, and directly recorded on an oscillograph. Typical examples of stress-wave emission (SWE) from a crack travering steel wires and boron fibers are shown in Fig. 7.[†] Noting the slight difference in time scale, there are at least an order of magnitude more SWE emanating from the boron fiber fracture. Although this is partly due to the fact that there were about twice as many boron fibers per unit fracture area, it can mostly be attributed to multiple breaks (5-10 typically) in the boron fibers as compared to single breaks in the steel wires.

Further correlation of SWE to stainless-steel wire fracture was obtained by comparing the load drops occurring during wire fracture to the stress waves. As noted in Fig. 8, each load drop was coincident with the occurrence of a large SWE. In some instances, two SWE occurred almost simultaneously which indicated two wires fracturing even though the load only dropped once. For two 10 percent volume fraction specimens, metallographic sectioning indicated a total of 54 fractured wires while SWE observations indicated a total of 52. The excellent correlation between these emitted waves and the wire fracture allowed determination of when the wires were failing. This permitted an average load and hence an average stress intensity factor to be associated with wire fracture. For example, in one specimen with a volume fraction of 0.10, K ranged from 70,500 to 86,000 psi-in$^{1/2}$ (249-303 kg/mm$^{3/2}$) for wire fracture.

[†]Testing of aluminum-boron composites is in the initial stages and is not reported. This one result was shown only for comparative purposes.

The average stress intensity and ℓ^* values associated with wire fracture are given in Table 1. Also given are the yield strength and secondary modulus of elasticity. The secondary modulus, E_c', is utilized since it is appropriate to a composite wherein the matrix is plastically yielding and the fibers are still elastic, except right at the crack tip. Experimental and theoretical justification for using E_c' is given elsewhere.[4] The fracture strain was then calculated from Eq. (4). This was compared to the measured fracture strains as taken from the observed wire diameters, e.g., as in Fig. 4. The measured fracture strain is obtained from

$$\epsilon_f = \ell n \left(\frac{A_o}{A_f}\right) \tag{9}$$

where A_o and A_f refer to original and final cross-sectional areas of the wires. For these measurements, some of the polishing planes were not mid-thickness and care was taken to reconstruct profiles so that reasonable estimates of fracture strains could be made.

In comparing ϵ^* and ϵ_f in Table 1, it is seen that in all cases the calculated value is somewhat larger than the measured value. However, the differences are not significant and in fact, for the 21 wires, the average calculated value of 1.07 is amazingly close to the average measured value of 0.93. In summary, the demonstration of a critical crack-tip displacement or fracture strain concept for a unidirectional composite has been presented. It is not unreasonable to assume that extension of similar concepts to finer-scale microstructures may be forthcoming.

REFERENCES

1. A. H. Cottrell, The Tewksbury Symposium on Fracture, C. J. Osborn, ed., Brown, Prior and Anderson, Ltd., (1965), p.1.

2. A. S. Tetelman and A. J. McEvily, Fracture of Structural Materials, John Wiley and Sons, Inc., New York, 1967.

3. W. W. Gerberich, Trans. AIME, 239 , May (1967), p. 753.

4. W. W. Gerberich, "Fracture in Metal-Metal Composites," Composite Materials: Fundamentals and Utilization, University of California, June (1968).

5. F. A. McClintock, J. Appl. Mech., Trans. ASME, 80, (1958), p.582.

6. W. W. Gerberich, Experimental Mechanics, November (1964), p. 335.

7. F. A. McClintock, ASTM Bulletin, April (1961), p. 277.

8. A. A. Wells, British Weld. J., 10 (1963), p. 563.

9. G. T. Hahn and A. R. Rosenfield, Acta Met., 13, (1965), p. 293.

10. J. E. Srawley and B. Gross, Materials Res. and Stnds., 7, April (1967), p. 155.

11. W. W. Gerberich and C. E. Hartbower, Int. J. Fracture Mechanics, 3, September (1967), p. 185.

TABLE 1: CALCULATED AND OBSERVED FRACTURE STRAINS

Volume Fraction V_f	Stress Intensity[(a)] K, psi-in$^{1/2}$ †	No. of wires in estimate	Yield Strength † σ_{ys}, psi	Secondary Modulus E_c', psi×10^{-6}†	Critical Distance† ℓ^*, in.	Fracture Strains Calc. ϵ^*(b)	Fracture Strains Meas. ϵ_f (c)
0.05	55,600	3	75,000	1.7	0.0041	1.87	1.52 (e) (1.45-1.58)[(d)]
0.10	74,200	7	99,500	3.69	0.0062	0.77	0.72 (.37-1.18)
0.10	81,800	8	99,500	3.69	0.0057	1.01	0.94 (.69-1.16)
0.20	144,000	2	133,000	6.66	0.0057	1.30	0.91 (.86-.96)
0.20	123,000	1	133,000	6.66	0.0068	0.80	0.55 (0.55)

(a) Average value for which wire fractures were observed.

(b) Calculated from Equation (4).

(c) Measured from diameters in micrographs using Eq. (9).

(d) Range

(e) Average

†Conversion Units:

1 psi = 7×10^{-4} kg/mm^2

1 psi-in$^{1/2}$ = 3.53×10^{-3} kg/mm$^{3/2}$

1 in. = 25.4 mm

LIST OF FIGURES

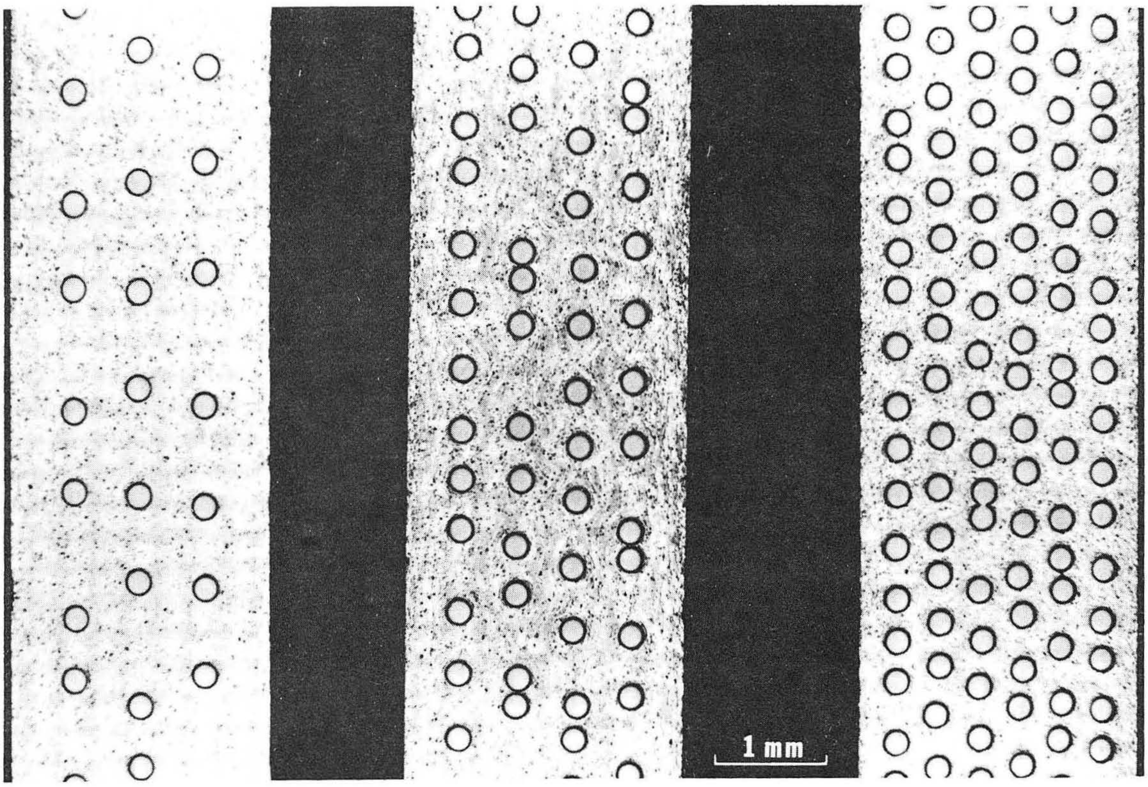

XBB 686-3412-A

Fig. 1

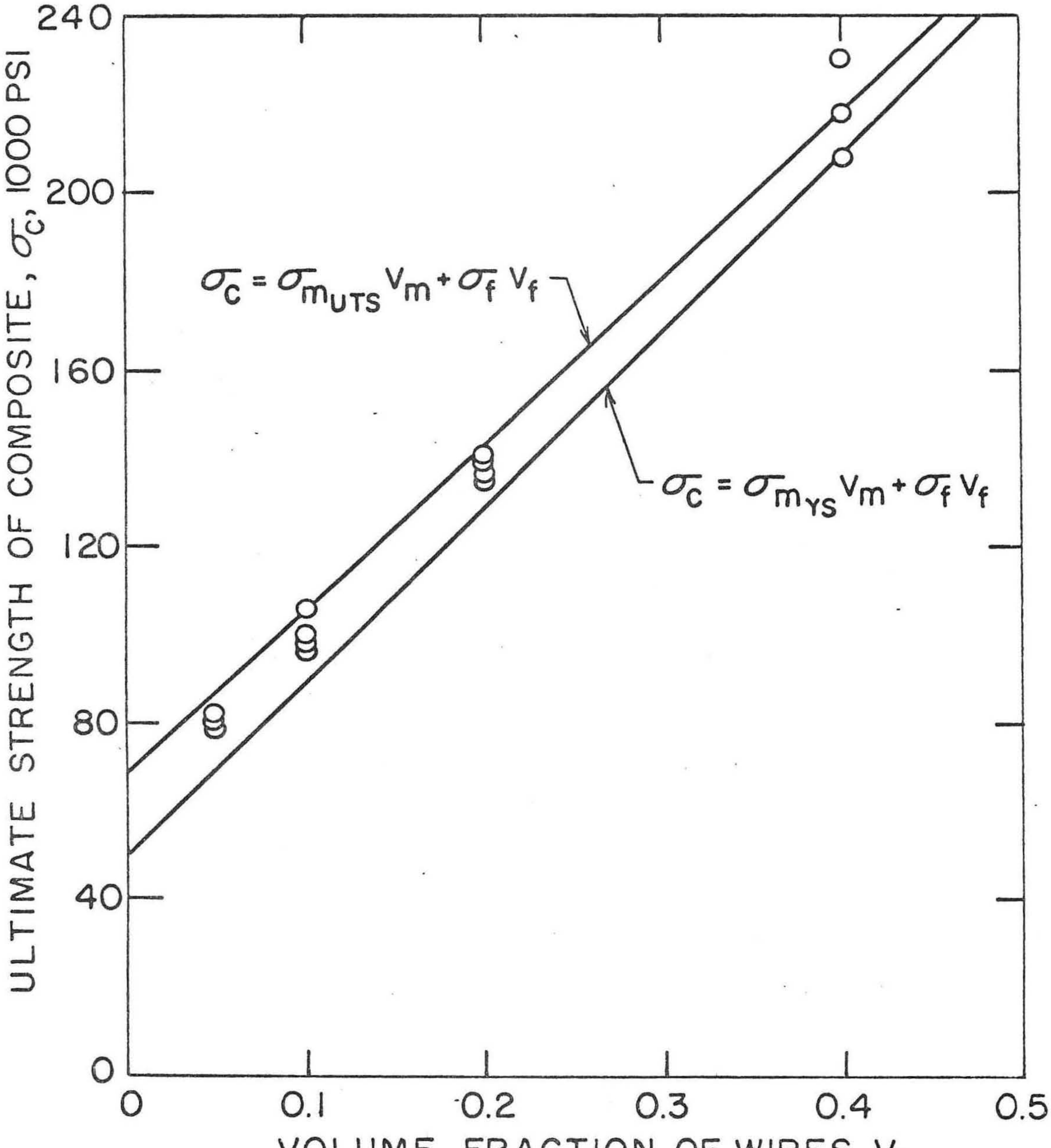

XBL 686-952-A

Fig. 2

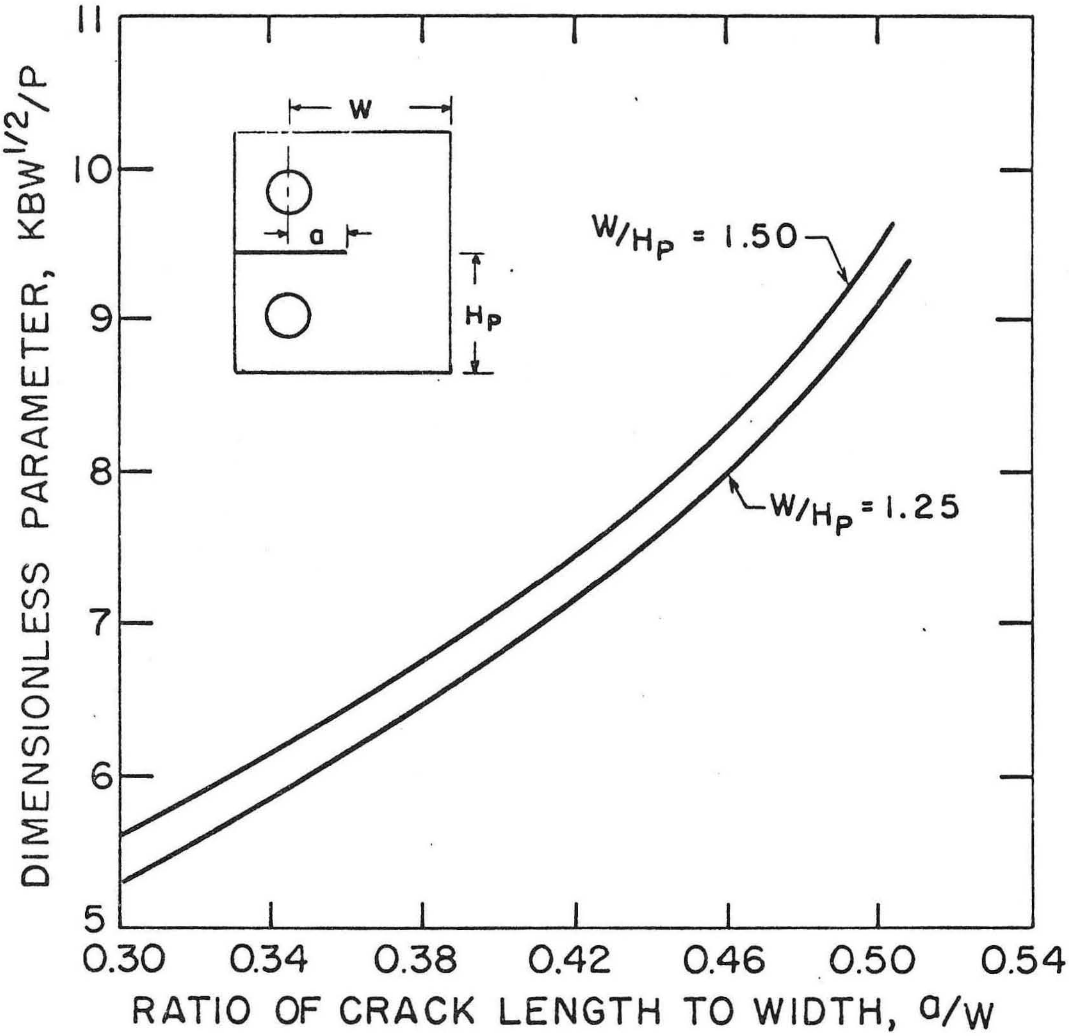

XBL 686-963

Fig. 3

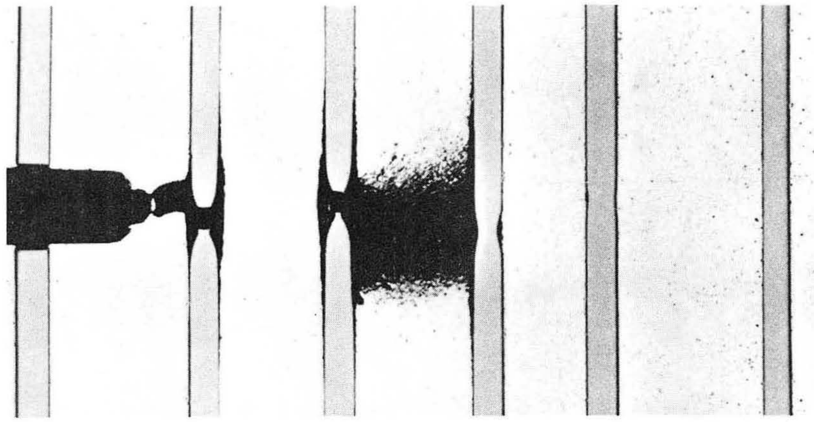

V_f = 0.05

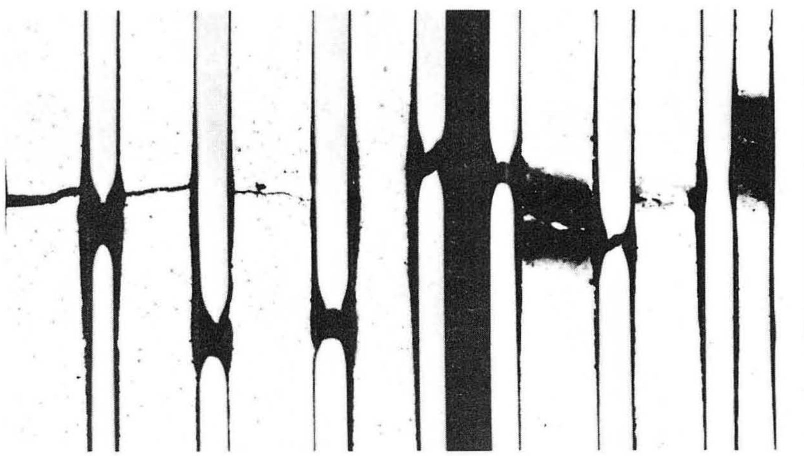

V_f = 0.10

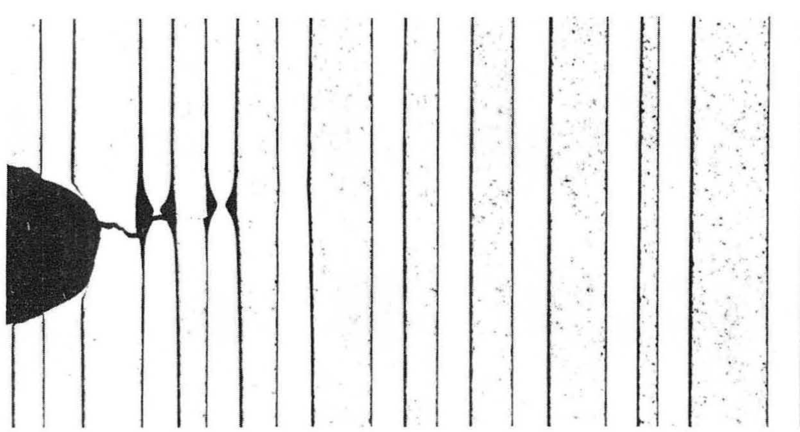

V_f = 0.20 1 mm

XBB 686-3411-A

Fig. 4

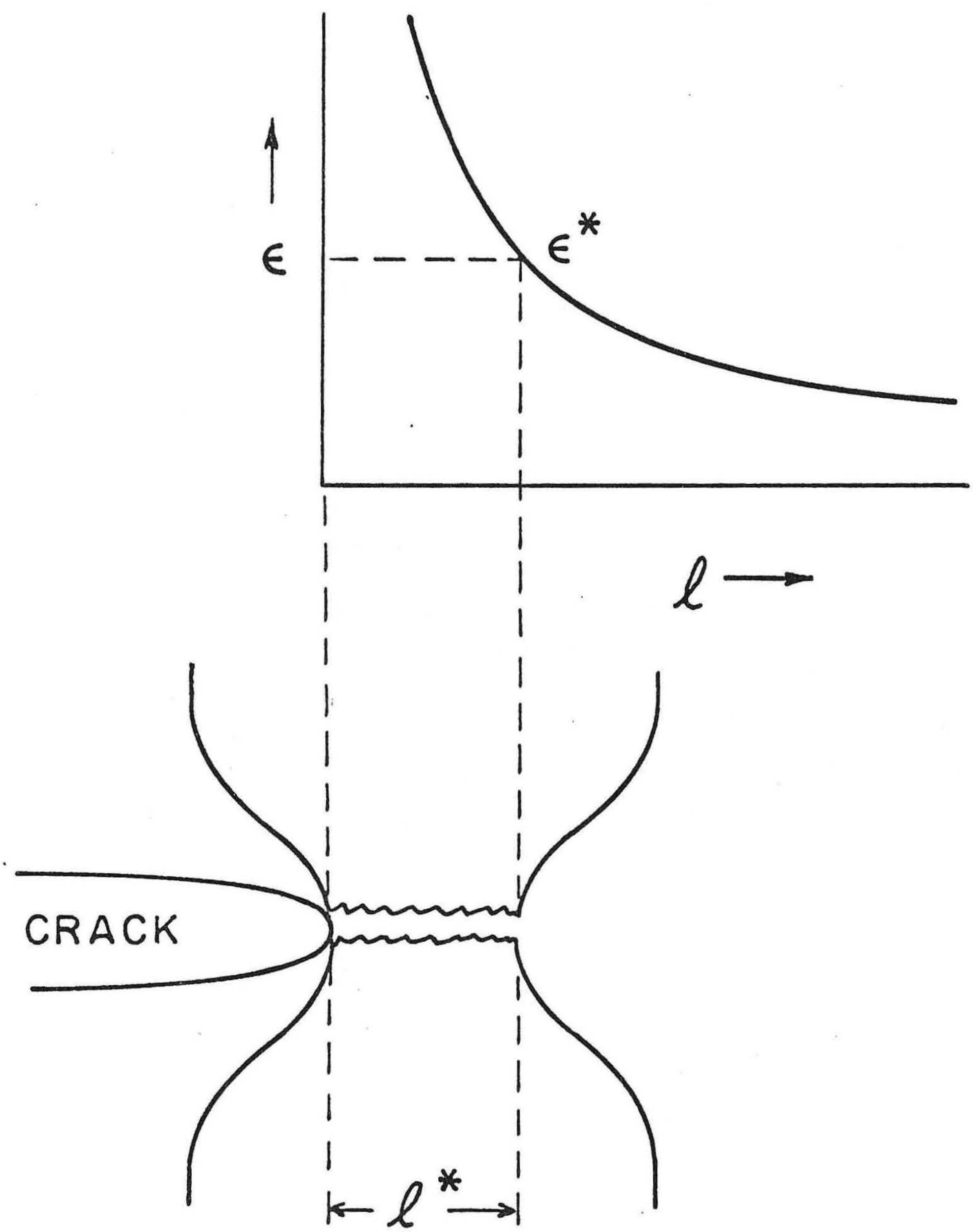

XBL 686-953

Fig. 5

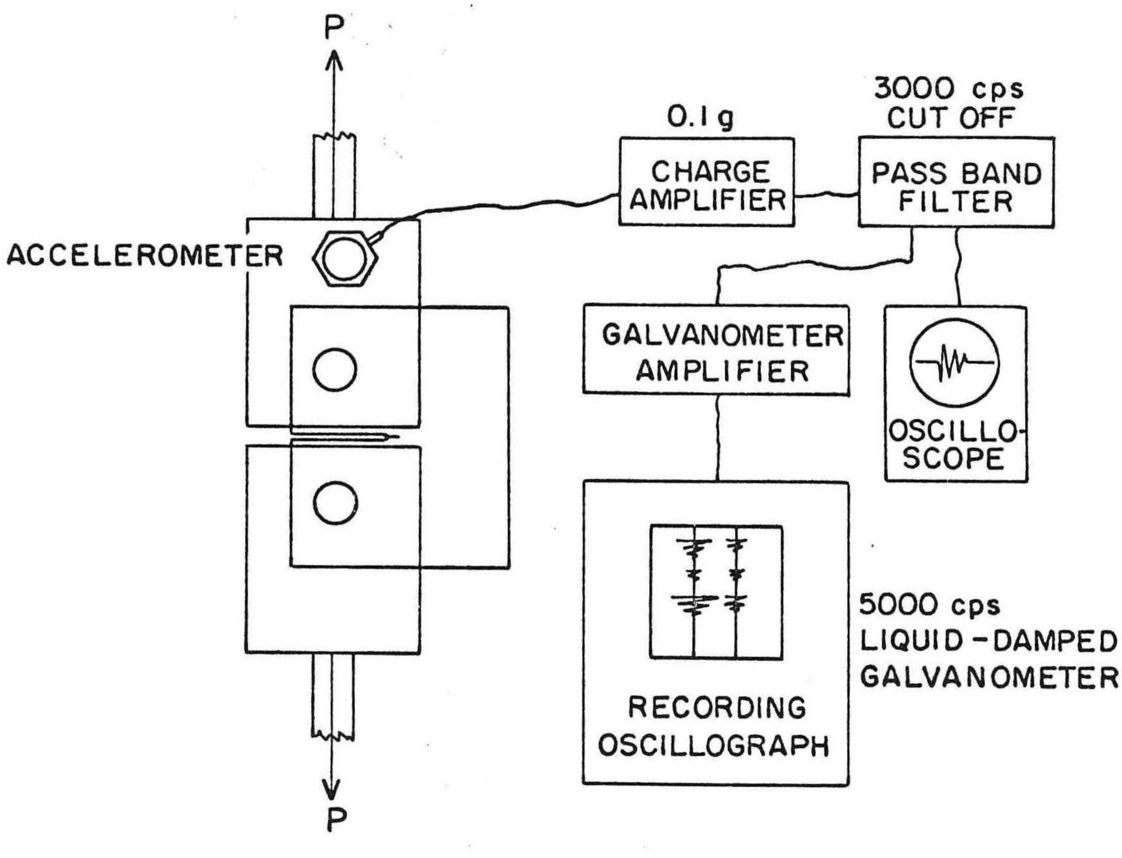

XBL 6812-6412

Fig. 6

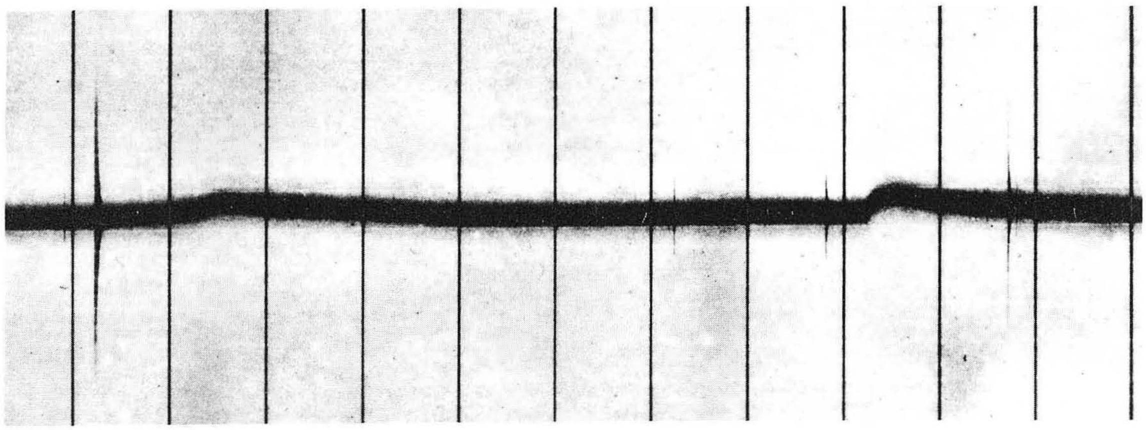

(a) SWE FROM STEEL WIRES 1 SECOND/DIVISION

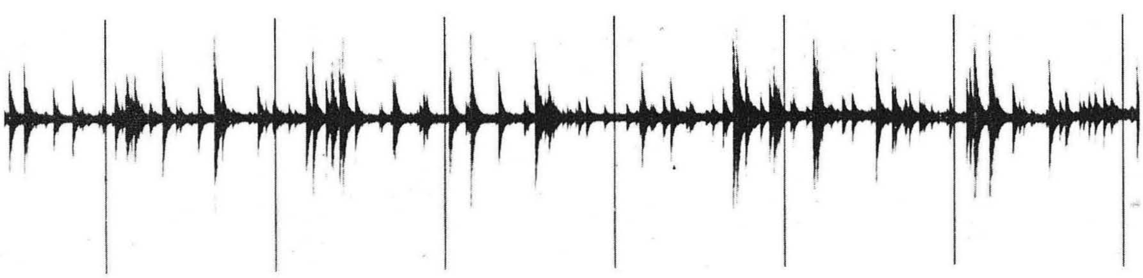

(b) SWE FROM BORON FIBERS 1 SECOND/DIVISION

XBB 6812-7644

Fig. 7

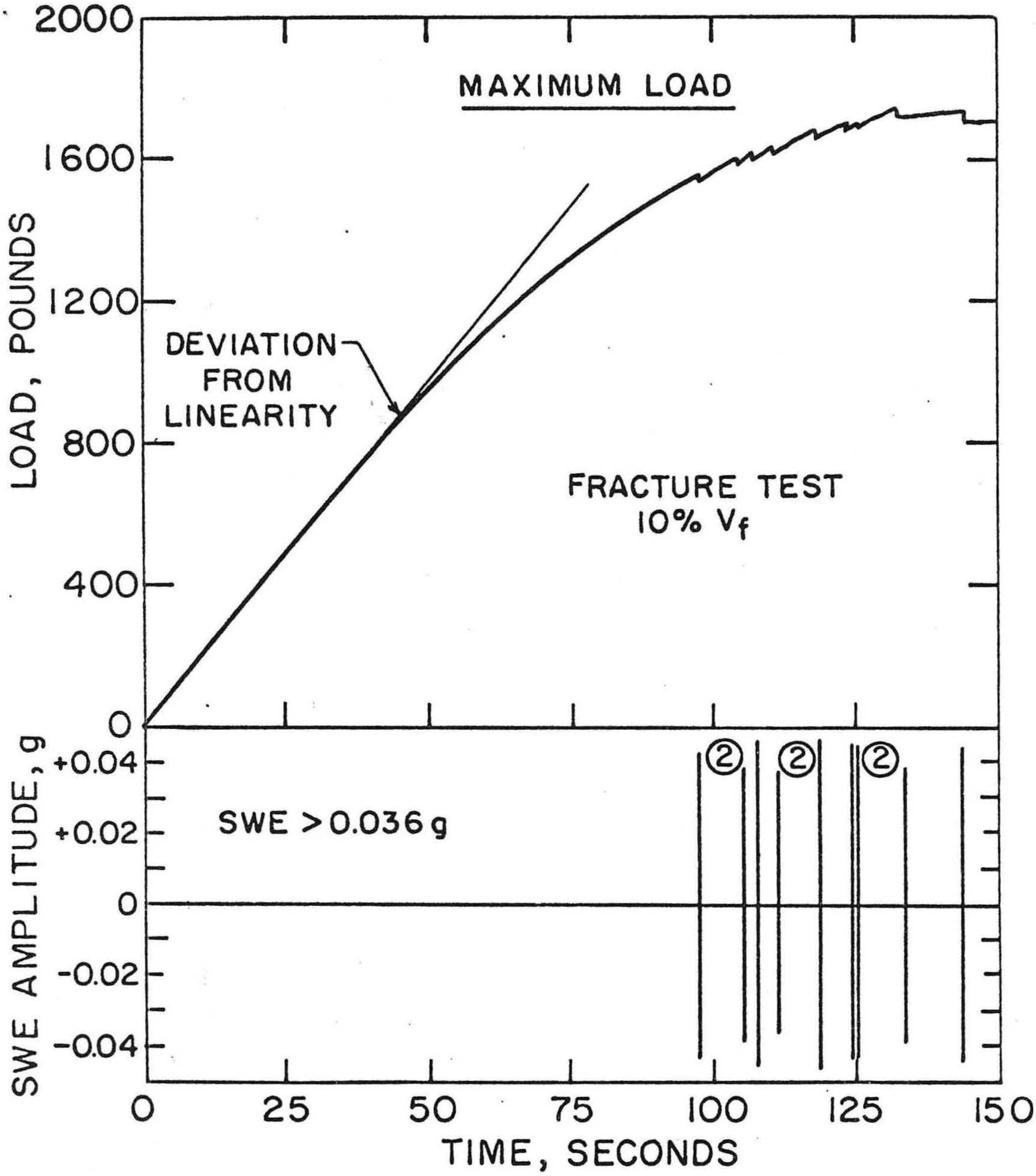

XBL 686-967

Fig. 8

TECHNICAL INFORMATION DIVISION
LAWRENCE RADIATION LABORATORY
UNIVERSITY OF CALIFORNIA
BERKELEY, CALIFORNIA 94720